

STRONG COMA LOBES FROM SMALL GRAVITATIONAL DEFORMATIONS

Sebastian von Hoerner
National Radio Astronomy Observatory*

ENGINEERING MEMO No. 140

*Operated by Associated Universities, Inc., under contract with the National
Science Foundation

Abstract

Short-wavelength beam mapping has produced very strong sidelobes at the 140-foot telescope, up to four lobes in a row when pointing far West. Various observations, and the theory of coma lobes, show in good agreement that the telescope suffers a large lateral defocussing, which varies by 7.25 cm EW and 2.8 cm NS for pointing changes of 90° . Since the lateral deformation of the feed support legs yields only 0.5 cm, it must be the optical axis which moves that much. This is achieved by a gliding rotation of the best-fit paraboloid, gliding along a slightly deformed surface, while rotating about the center of the average surface curvature, located somewhat higher than $2F$ above the vertex. The resulting lateral focal offset can be much larger than the causing rms surface deformation, up to 47.3 times for our focal ratio. This gliding rotation is confirmed by a structural analysis. It is to be expected at many telescopes, whenever the rim is more flexible than the center, and the resulting degradation of efficiency and beamshape will be significant if gravity is important in the error budget. In these cases the telescope should be supplied with a variable lateral shift of the focal mount, computer-controlled as a function of the pointing, following the axial movements. This additional degree of freedom will improve the short-wavelength performance considerably for telescopes whose surface panels excel the gravitational behavior.

I. Introduction

Gravitational degradations of efficiency and beamshape of the 140-ft telescope, and an East-West asymmetry of these effects, have been reported by several observers during the last years, when observations went to short wavelengths of a few centimeters. The strongest mode of gravitational deformation,

the astigmatism, was predicted from structural reasons [1], measured with an elongated feed horn [2], and partly corrected for with a deformable sub-reflector [3]. But of this last reference, Figure 4 and its discussion showed clearly that in addition to the astigmatism we must have some other strong mode of degradation, having its minimum value not on the meridian but 1-2 hours East, and causing strong sidelobes for extreme hour angles, especially far West. The degradation and its EW-asymmetry were also found in recent measurements of the aperture efficiency as a function of pointing angles, for both prime focus [4] and Cassegrain focus [5].

The strong sidelobes, up to four at 22 GHz, looked like coma lobes caused by lateral defocussing. But this needed a feed offset of about 7 cm which at first seemed impossible for two reasons: the feed legs could not deflect that much under their known load and stiffness, and a deflection of 7 cm would cause a pointing deviation of about 12 arcmin while our largest observed pointing parameters are only about 2 arcmin.

The present investigation will show that we have indeed coma lobes from a lateral offset between the feed (or Cassegrain mirror) and the optical axis, but that it is mainly the axis of the best-fit paraboloid which moves sideways at large hour angles, and not so much the feed legs; and in this case the pointing deviation is only small, about 2 arcmin. The EW-asymmetry is just an unfortunate misalignment of the surface or the receiver box mount.

II. The Observations

First, when the deformable subreflector was tested [3], many beam maps were taken at 22.3 GHz ($\lambda = 1.345$ cm). An example is given in Figure 1, showing the strong sidelobes at large hour angles, while the hour angle of the

most symmetric and round beam, H_o , is about 2 hours East (negative). Seven observed sources with declinations $-28^\circ \leq D \leq +62^\circ$ yield, independent of D ,

$$H_o = -1^h 44^m \pm 05^m, \text{ for Cassegrain mirror.} \quad (1)$$

During the same set of observations, a smaller but still significant North-South effect was found, as shown in Figure 2. Investigating (close to H_o) the NS-asymmetry of the beam for all sources, we find by linear regression that the best beamshape is obtained at the declination

$$D_o = +10^\circ \pm 3^\circ, \text{ for Cassegrain mirror.} \quad (2)$$

This is at elevation $E = 62^\circ$ on the meridian. The 140-ft surface was readjusted in 1972 for an intended best performance at $E = 60^\circ$ on the meridian, and the measured astigmatism was found zero at $E = 53^\circ$ [2]. Thus, the last adjustment was done well in declination but off in hour angle.

Second. If the observed EW-degradation is caused by lateral defocussing, then an offset feed should give better performance than a centered one for certain hour angles. This was tested together with P. Crane in May 1979 with an available two-feed receiver at $\lambda = 2.04$ cm; one feed is at the center of the Sterling mount while the second feed is offset by a feed separation of $x_2 = 3$ inch = 7.62 cm. A result is shown in Figure 3, confirming the expectation. A large number of maps yield for the centered feed, independent of declination,

$$H_o = -1^h 06^m \pm 09^m, \text{ for prime focus.} \quad (3)$$

This is significantly different from (1) which means that the Cassegrain mount has some East-offset of its own.

These two-feed observations yield three additional useful cases of symmetry. The offset feed, East of the center, gives a symmetric and round beam at $H_1 = + 4^h 22^m \pm 12^m$, and both beams are mirror-symmetric to each other (with their sidelobes in between) at $H_2 = + 1^h 40^m \pm 15^m$. With the offset feed to the West, a round beam cannot be achieved even at most eastern pointings, and the case of mirror-symmetry occurs at $H_3 = - 2^h 28^m \pm 12^m$. We call x the linear offset (plus is West) of the Sterling center from the best-fit optical axis, and we now assume that the dependence of x on hour angle is caused by the x -component of gravity (parallel to the declination axis),

$$x = x_0 (\sin H - \sin H_0) \quad (4)$$

with two unknown parameters, x_0 and H_0 , where x_0 must be the same for prime focus and Cassegrain while H_0 may be different. Including (3), measuring x in centimeter, and using $x_2 = 7.62$ cm, we write all four cases of symmetry as

$$\begin{aligned} \sin H_0 &= -0.284 \\ \sin H_0 + 7.62/x_0 &= \sin H_1 \\ \sin H_0 + 3.81/x_0 &= \sin H_2 \\ \sin H_0 - 3.81/x_0 &= \sin H_3 . \end{aligned}$$

This is a set of four linear equations for the two unknowns $\sin H_0$ and $1/x_0$.

The solution and its mean error are

$$H_0 = - 0^h 35^m \pm 14^m , \quad \text{for prime focus,} \quad (5)$$

$$x_0 = 7.25 \text{ cm} \pm .19 \text{ cm,} \quad \text{for prime and Cassegrain.} \quad (6)$$

If the difference between (5) and (3), $\Delta H_0 = 31^m \pm 17^m$, is real, it indicates some other gravitational mode, in addition to lateral defocussing.

The lateral offset at zenith pointing ($H = 0$) follows from (1), (3) and (6) as

$$x_{zen} = -x_o \sin H_o = \begin{cases} + 3.18 \text{ cm} \pm .43 \text{ cm, for Cassegrain mirror,} & (7) \\ + 1.10 \text{ cm} \pm .45 \text{ cm, for prime focus.} & (8) \end{cases}$$

Third. The aperture efficiency was measured by R. Brown at prime focus, $\lambda = 2.82 \text{ cm}$ [4], and with the deformable Cassegrain, $\lambda = 1.345 \text{ cm}$ [5]. We call H_m the hour angle of maximum efficiency. If lateral defocussing were the only degradation, then $H_m = H_o$ and independent of D . If only astigmatism were added, then $H_m \approx H_o$ for $10^\circ \leq D \leq 70^\circ$ where astigmatism is small, while $H_m \rightarrow 0$ far South where astigmatism dominates. The observations show this approach to zero for both Cassegrain and prime focus. For the most relevant range of $10^\circ \leq D \leq 30^\circ$, they give

$$H_m = \begin{cases} - 1^h 42^m \pm 12^m, & \text{for Cassegrain mirror,} & (9) \end{cases}$$

$$H_m = \begin{cases} - 0^h 46^m \pm 15^m, & \text{for prime focus,} & (10) \end{cases}$$

where (9) agrees with (1), and (10) with (3) and (5). But further North, H_m still decreases, below -2^h , which again indicates additional degradations.

Fourth. The telescope surface was measured in zenith pointing with a new method by J. Findlay in October 1978 [6], with simultaneous sightings from the surface vertex to the Sterling center. The offset of the Sterling center from the axis of the best-fit paraboloid was then found by L. King, in agreement with (8), as

$$x_{zen} = + 1.05 \text{ cm} \pm .26 \text{ cm, for prime focus.} \quad (11)$$

III. Comparison with Theory of Coma Lobes

The observations, especially those with the two-feed receiver, lead to the conclusion that the 140-ft suffers a strong lateral feed offset as a function

of pointing angle. But so far we have used only beam symmetries or efficiency maxima, but not any details of the well pronounced sidelobe pattern. Since a pattern of coma lobes is easily calculated, we decided to do so.

Experiments with the deformable subreflector have shown that the astigmatism has a strong influence on height and shape of sidelobes, but only a small influence on their location. We thus shall limit the calculations to the cardinal scan angle (parallel to the feed offset) which intersects all coma lobe maxima, yielding their locations.

The aperture is described in polar coordinates, with $r = 1$ (nondimensional) at the rim, and with $\alpha = 0$ in direction of the feed offset. We call $F =$ focal length, $d =$ aperture diameter, $\Phi = F/d$, and $k = 1/(4\Phi)^2$. We use the normalizations

$$L = \frac{x}{2\lambda\Phi}, \quad \text{with } x = \text{lateral feed offset (off axis);} \quad (12)$$

$$G = \frac{Y}{2\lambda/d}, \quad \text{with } \gamma = \text{scan angle (off source).} \quad (13)$$

Using equations (2) and (11) of reference [7], the phase lag at the feed of a ray from (r, α) is $\phi = \zeta \cos \alpha$, with

$$\zeta = 2\pi \left\{ G + \frac{L}{1+kr^2} \right\} r. \quad (14)$$

The voltage amplitude then is

$$A(G, L) = 2 \int_{r=0}^1 r dr f(r) \int_{\alpha=0}^{\pi} \cos(\phi) d\alpha = 2\pi \int_{r=0}^1 f(r) J_0(\zeta) r dr. \quad (15)$$

The received power is $P = A^2$, and J_0 is the Bessel function of zero order. For the power illumination of the aperture we use $f^2 = 1 - tr^2$ with 13 db edge taper, fitting our receivers, and we use $\Phi = 0.4286$ for the 140-ft. Equation (15) was integrated numerically for offsets $L = 0, 1, 2, \dots, 15$, scanning in G through the

main beam ($m=0$) and the first 5 sidelobes ($m = 1, 2, \dots 5$), solving for their location G_m and power P_m . The angular separation of the m -th lobe from the main beam we call

$$\Delta G_m = G_m - G_0. \tag{16}$$

The results show, first, that the powers P_m are not a good measure for the offset L . For example, P_1/P_0 can theoretically never be more than 0.20 (for $L = 6.5$), whereas it is actually 0.67 in Figure 1,a which is mainly caused by astigmatic degradation of the main beam, as shown in Figure 3 of Reference [3]. Furthermore, the calculated internal ratios, P_2/P_1 , P_3/P_2 and so on, are rather insensitive to L for small L and ambiguous for large L .

Second, for $m \geq 2$, the angular lobe separations $\Delta G_m(L)$ may be used for confirming that we have indeed coma lobes, and for a rough estimate of L and thus of H_0 and x_0 . This is done in Figure 4 for the first set of (Cassegrain) observations, treating a total of 79 beam maps, and showing qualitative agreement but obvious deviations. The second set (two-feed at prime focus) is treated the same way. Using the number n of all lobes $m \geq 2$ for a numerical evaluation, the best-fitting values and their mean errors are

	n	H_0	x_0 (cm)	x_{zen} (cm)	
Cassegrain	102	$-0^h 38^m \pm 15^m$	10.6 ± 1.2	$1.7 \pm .7$	(17)

Prime focus	16	$-0^h 48^m \pm 27^m$	10.1 ± 1.6	2.1 ± 1.2	(18)
-------------	----	----------------------	----------------	---------------	------

In spite of their large mean errors, these values do not agree with our previous results. Detailed inspection shows that this is mainly caused by the few right-hand lobes (Figure 1,a) observing far East where astigmatism plays a stronger role. Using only the left-hand lobes (Figure 1,c) we obtain satisfactory agreement:

	n	H _o	x _o (cm)	x _{zen} (cm)	
Cassegrain	92	-2 ^h 07 ^m ± 56 ^m	7.4 ± 1.8	3.9 ± 1.9	(19)
Prime focus	12	-1 ^h 15 ^m ± 44 ^m	8.9 ± 1.9	2.9 ± 1.8	(20)

Third, regarding the North-South-effect (Figure 2), we have no sidelobes $m \geq 2$, which would require shorter wavelengths. For a rough estimate we use the height of the first sidelobe or shoulder; not directly, for the reasons given above, but only as compared to the height of the EW-effect, assuming the same degradations for both. We omit a detailed description of this procedure because the NS-effect turns out to be small. We assume that its lateral offset y is caused by the y -component of gravity (perpendicular to optical and declination axes). Close to the meridian, this means

$$y = y_o \{ \sin(D - \ell) - \sin(D_o - \ell) \} \quad (21)$$

where $(D - \ell)$ is the zenith distance, $\ell = 38.4^\circ$ the geographical latitude of Green Bank, and $D_o = 10^\circ$ from (2). The investigation of 16 beam maps (first set of observations), close enough to H_o for showing the NS-effect best, gives

$$y_o = 2.8 \text{ cm} \pm 0.3 \text{ cm} \quad (22)$$

and for zenith pointing ($D = \ell$)

$$y_{zen} = 1.3 \text{ cm} \pm 0.3 \text{ cm, for Cassegrain mirror.} \quad (23)$$

For comparison, the analysis of J. Findlay's measurements of the surface [6] gives

$$y_{zen} = + 0.4 \text{ cm} \pm 0.2 \text{ cm, for prime focus.} \quad (24)$$

This seems significantly different from (23), indicating some additional N-offset of the Cassegrain mount.

IV. Gliding Rotation of the Best-Fit Paraboloid

The observations show a large lateral feed offset when the telescope is tilted, and, as seen from the optical axis, the feed moves away in the direction of gravity, for both the EW and the NS effect. This seems to indicate gravitational deformations of the feed support legs as an explanation, giving the proper direction. But it must be ruled out as the main cause for three reasons. First, structural symmetry of the legs demands equal deformation under equal forces in all directions, EW and NS, which is clearly not the case. Second, a feed movement x_0 gives a pointing deviation of $p = B x_0 / F = 11.5$ arcmin ($B = 0.844 =$ beam deviation factor), whereas the largest pointing parameters of the 140-ft are only 2 arcmin. Third, calculations of stiffness and load yield a lateral apex movement relative to the backup structure of only 0.5 cm which is too small.

If it is not the feed, it must be the optical axis which moves. The movement of the best-fit paraboloid must be such that small gravitational surface deformations Δz , of a few millimeters, can cause a large axial movement x_0 , which calls for a special type of deformation. We call $\sigma = \text{rms}(\Delta z)$, averaged over the aperture, and $Q = x_0 / \sigma$. The demand of large Q then leads to the "gliding rotation" explained in Figure 5. If the surface deformations were exactly of this type (no additional degradations), then the telescope would have one of the homologous deformations [8] where one paraboloid is just deformed into another paraboloid, as it is approximated by recent designs.

The vertex of a paraboloid may be defined as its point of maximum curvature. If the rim is more flexible than the central parts (see Figure 5,b), then lateral gravity will make the rim (relative to the center) straighten down at one side but curve up at the other, which shifts the point of maximum curvature toward

that side which curves up, and the vertex then is shifted by an amount Δv in the direction opposite to gravity. Since the feed legs deform in the direction of gravity, both effects add up for the offset between feed and axis. This gliding rotation and its resulting lateral defocussing are to be expected at most radio telescopes, whenever the rim is more flexible than the center; and the resulting degradations of beamshape and gain will actually be felt whenever gravity plays an important role in the error budget of the surface. The telescope then should get a new focal mount allowing a variable computer-controlled lateral movement.

A parabolic surface has, for the vertex, its center of curvature at height $2F$ above the vertex. If the best-fit paraboloid rotates about this point, then $\Delta z = 0$ for the surrounding of the vertex and still small elsewhere, with a maximum at the rim where $x_o/\Delta z_{rim} = (4\phi)^3$ as can be shown, with $\phi = F/d$. We omit lengthy but straightforward derivations. Averaged over the whole aperture, a rotation about $2F$ gives

$$Q_o = \frac{1}{\sqrt{5}} (8\phi)^3. \quad (25)$$

But we see from Figure 5 that the best point of rotation for minimizing σ would not be at $2F$, the center of vertex curvature, but slightly higher, at the average center of curvature. We call its height $(2+q)F$. For any given ϕ , the value of q for maximum Q is found by a least-squares procedure as

$$q = \frac{2\psi + 5}{\psi(2 + \psi)} \quad (26)$$

where $\psi = (8\phi)^2$, and this maximum of Q then is $Q = KQ_o$ with Q_o of (25) and

$$K = \frac{1 + q}{\sqrt{1 - \frac{4}{5} (q\psi) + \frac{1}{5} (q\psi)^2}} \quad (27)$$

TABLE 1.

Gliding rotation about a point $(2+q)F$ above the vertex.
 For a given focal ratio ϕ , the calculated value of q will
maximize the relative axial offset $Q = x/(\text{rms } \Delta z)$.

$\phi = F/d$	$Q_o = Q(o)$	q	$Q(q)$
0.30	6.18	.370	18.8
.35	9.82	.268	27.7
.40	14.7	.204	39.3
.4286	18.0	.176	47.3
.45	20.9	.159	54.0
.50	28.6	.128	72.1
.70	78.5	.0648	186.9
1.00	229.0	.0314	528.1
∞	$(8\phi)^3/\sqrt{5}$	$2/(8\phi)^2$	$(8\phi)^3$

This gliding rotation of the best-fit paraboloid, gliding along a slightly deformed surface, is able to give an adequate explanation of the observations, which the feed leg deformation could not give. First, it is now expected that the EW-effect is larger than the NS-effect: Figure 5b explains that the rotations are caused by the difference in stiffness between rim and central backup structure; the rim is about equally flexible in any direction, but the central backup structure is stiffer EW than NS (because of the rigid declination axis) as was shown by the observed astigmatism of the telescope [2], thus the stiffness difference is larger EW than NS. Second, the resulting pointing deviation is now only $p = (1-B) x_o/F = 2.1$ arcmin, see Figure 5a, in agreement with our pointing parameters. Third, we see from Table 1 that the lateral feed offset can indeed be much larger than the surface deformations, up to 47 times for the 140-ft, and extremely large for long focal ratios.

V. Structural Analysis

With a computer model of the 140-ft, deformations and best-fit paraboloid were analyzed by W.-Y. Wong, with gravity in x-direction (EW-effects) and y-direction (NS-effects), where the full gravity works NS but only its fraction $\cos \ell = 0.784$ works EW, at latitude $\ell = 38^\circ 4'$. Because of its irrelevance to performance, we subtract from the computer data a rigid-body movement, obtained from the structural center, of 0.20 cm translation and 1.1 arcmin rotation. The maximum rim deformation then is only $\Delta z = 0.36$ cm. The feed support legs deform by $s = 0.48$ cm (EW) and $s = 0.61$ cm (NS) at the focus. The total offset ξ between feed and optical axis is

$$\xi = \begin{cases} x_0 = 5.05 \text{ cm, EW,} \\ y_0 = 2.91 \text{ cm, NS.} \end{cases} \quad (28)$$

The fraction of the offset caused by surface deformations then is

$$\tau = \xi - s = \begin{cases} 4.57 \text{ cm, EW,} \\ 2.30 \text{ cm, NS.} \end{cases} \quad (29)$$

We consider (28) as being in qualitative agreement with the observation (6) and (22), confirming our assumption of coma lobes from large lateral defocussing, and we ascribe the quantitative differences mainly to the somewhat awkward 140-ft structure (many short thick members) which is difficult to model for the computer, especially because a gliding rotation is defined only by the second derivative (curvature) of the surface deformations.

Next, we want to check on our assumption of a gliding rotation. In the analysis, the best-fit paraboloid shows a vertex shift Δv (Figure 5,a) and an axial rotation $\Delta \alpha$ of

	Δv	$\Delta\alpha$	$F \Delta\alpha$	
EW	7.92 cm	6.67 arcmin	3.55 cm	(30)
NS	4.32 cm	3.75 arcmin	1.99 cm	

If offset τ and vertex shift Δv are caused by a gliding rotation about a point at height $(2+q)F$, we expect $\tau = (1+q)F \Delta\alpha$, and $\Delta v = (2+q)F \Delta\alpha$, from which q follows as

from	follows	EW	NS	
feed offset τ	$q = \tau / (F \Delta\alpha) - 1 =$	0.29	0.15	} $\bar{q} = 0.21 \pm 0.03$ (31)
vertex shift Δv	$q = \Delta v / (F \Delta\alpha) - 2 =$	0.23	0.17	

The results confirm that we have indeed a gliding rotation about a point somewhat above $2F$, fairly close to the point with the optimum value of $q = 0.176$ for maximum Q from Table 1.

VI. Conclusions

The results of various astronomical observations, of the theory of coma lobes and of the structural analysis (together with the explanation of a gliding rotation) show enough agreement to conclude that a considerable degradation of the telescope is due to a large lateral defocussing. When the pointing angle changes by 90° , the focal offset moves by 7.25 cm EW and by 2.8 cm NS; the offset is zero at hour angle $H_o = -1^h 44^m$ and declination $D_o = 10^\circ$. It is suggested to avoid this degradation by a mechanical lateral movement of the focal mount.

As a first and fast step, a fixed lateral shift is suggested for moving the zero offset to the best pointing angle. It should be on the meridian, $H_o = 0$, for an EW-symmetric performance, which according to (7) means a shift of 3.2 cm East, because observations at short wavelengths will be done with the Cassegrain

mirror. The present value of D_o gives more degradation North than South (Figure 2). We demand equal degradations at 15° above horizon ($D = -36.6^\circ$) and at 15° South of the pole ($D = +75^\circ$); with (21) this yields $D_o = 28^\circ$ as the best pointing for the zero offset, and with (22) we obtain the needed shift as 0.8 cm South. With these fixed shifts, the maximum lateral offsets then are, for $+6^h$ hour angle and for 15° elevation or 75° declination,

$$\xi = \begin{cases} \pm 7.25 \text{ cm, EW,} \\ \pm 2.18 \text{ cm, NS.} \end{cases} \quad (32)$$

The second step is a variable lateral shift of the focal mount, computer-controlled as a function of the pointing, with a range as given by (32). This is a large project, to be recommended only if well justified, for which we suggest the following procedure: calculate the gain loss due to the lack of a variable shift; find the random rms surface error δ which would produce the same loss; and compare this to the actually prevailing rms surface error ϵ from maladjustment and bumpiness of the surface panels.

The numerical integration of (15) leads to a good approximation (for $L \leq 6$) for the peak power of the main lobe

$$P_o = e^{-0.02702 L^2} \quad (33)$$

with $L = \xi / (2\lambda\phi)$, whereas a random rms surface error δ would give, for $\phi = 0.4286$ according to Ruze [9],

$$P_o = e^{-0.76(4\pi\delta/\lambda)^2}. \quad (34)$$

This yields in general, and with the offsets ξ from (32),

$$\delta = \frac{\xi}{57.1} = \begin{cases} 1.27 \text{ mm, EW,} \\ 0.38 \text{ mm, NS.} \end{cases} \quad (35)$$

According to J. Findlay's measurements, the actual surface errors are

$$\epsilon = \begin{cases} 1.2 \text{ mm, at present (maladjustment and bumpiness),} \\ 0.7 \text{ mm, after perfect adjustment (bumpiness only).} \end{cases} \quad (36)$$

Comparison of (35) and (36) yields the conclusions that the variable EW-shift is highly recommended for the present surface, and would be vital after readjustment; whereas the variable NS-shift can be omitted, even after readjustment. But the variable NS-shift would be needed, too, if the telescope were ever to be resurfaced.

REFERENCES

- [1] S. von Hoerner and W.-Y. Wong, "Gravitational deformation and astigmatism of tiltable radio telescopes," IEEE Trans. Antennas Propagat., vol. AP-23, p. 689, 1975.
- [2] S. von Hoerner, "Measuring the gravitational astigmatism of a radio telescope," IEEE Trans. Antennas Propagat., vol. AP-26, p. 315, 1978.
- [3] S. von Hoerner and W.-Y. Wong, "Improved efficiency with a mechanically deformable subreflector," IEEE Trans. Antennas Propagat., vol. AP-27, 720, 1979.
- [4] R. L. Brown, "High frequency performance of the 140-ft telescope, I.: Observations at 10,650 MHz." NRAO Engineering Memo No. 132, Feb. 1979.
- [5] R. L. Brown, "High frequency performance of the 140-ft telescope, II.: Observations at 22,235 MHz." NRAO Engineering Memo No. 133, Oct. 1979.
- [6] J. W. Findlay, "Measuring the surface of the 140-foot," NRAO Engineering Memo No. 129, March 1979.
- [7] S. von Hoerner, "Telescope surface measurement with two feeds," IEEE Trans. Antennas Propagat., vol. AP-26, p. 857, 1978.
- [8] S. von Hoerner, "Homologous deformations of tiltable telescopes," J. Struct. Division, Proc. Am. Soc. Engrs. vol. 93, p. 461, 1967.
- [9] J. Ruze, "Antenna tolerance theory," IEEE Proceedings, vol. 54, p. 633, 1966 (Figure 7).

FIGURE CAPTIONS

Fig. 1. 140-ft beam mapping at $\lambda = 1.345$ cm (22.3 GHz), with unresolved point source (Ori A, Declination = $-5^{\circ}4$), showing strong EW-effect of sidelobes and asymmetry. H = hour angle, E = elevation. Contour lines in geometric progression at 1, 2, 4, 8, ... K of antenna temperature; numbers shown are peak values. Cassegrain focus.

- a) Observing far East: strong right-hand sidelobe;
- b) Symmetric beam not on meridian, but about 2^{h} East of it;
- c) Observing far West: strong left-hand sidelobes.

Fig. 2. Beam mapping as in Fig. 1, showing weak NS-effect. Given are source name, declination D, hour angle H, and elevation E. Selected are some of those maps which are closest to the hour angle of EW-symmetry where NS-effects can be seen best.

- a) Observing far North: southern sidelobe;
- b) Best NS-symmetry at about $+14^{\circ}$ declination;
- c) Observing far South: northern shoulder.

Fig. 3. Beam mapping with a two-feed receiver at prime focus, $\lambda = 2.04$ cm (14.7 GHz). The source is 3C 84, at declination D = $+41^{\circ}3$, observed at H = $+3^{\text{h}} 04^{\text{m}}$ West. At this hour angle, the offset feed gives a better performance than the centered feed.

- a) Offset feed, at 7.62 cm East of center; peak = 74 K.
- b) Feed at center of Sterling mount; peak = 62 K, sidelobe = 10 K.

Fig. 4. Separation of sidelobes, observation (---) and theory (—).

Open symbols for left-hand lobes observing West of H_0 , filled symbols for right-hand lobes observing East of H_0 . Used are $H_0 = -0^{\text{h}} 38^{\text{m}}$ and $\xi_0 = 10.58$ cm, the best-fit values for this graph. Same observations as Fig. 1.

L = lateral feed offset, normalized with equation (12).

ΔG_m = angular distance of m-th sidelobe from main beam, see equations (13) and (16).

Fig. 5. Gliding rotation of the best-fit parabola, within a slightly deformed surface (---), rotating here about the point $2F$ on the axis.

- a) Small deformations Δz can cause a large feed offset x ; but the resulting pointing deviation $p = (1-B)\Delta\alpha$ is still small (B = beam deviation factor).
- b) This effect will take place whenever the rim is more flexible than the central part of the backup structure.

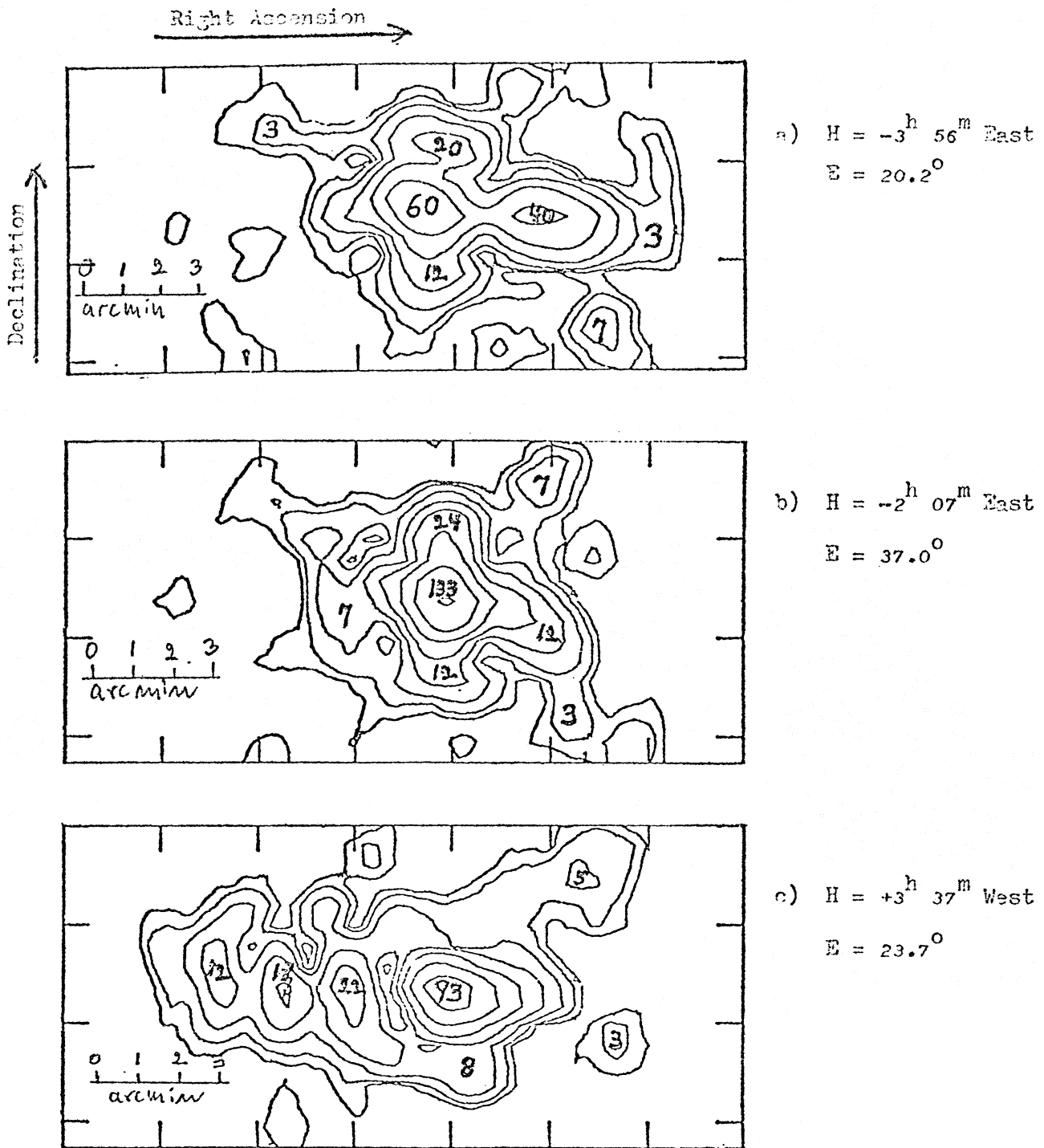
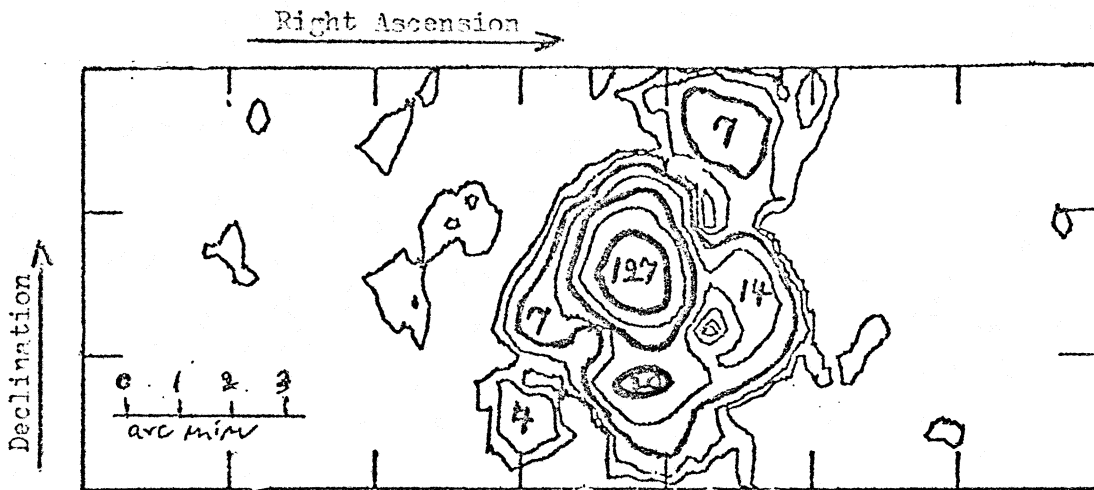


Fig. 1. 140-ft beam mapping at $\lambda = 1.345$ cm (22.3 GHz), with unresolved point source (Ori A, Declination = -5.4°), showing strong EW-effect of sidelobes and asymmetry. H = hour angle, E = elevation. Contour lines in geometric progression at 1, 2, 4, 8, ... K of antenna temperature; numbers shown are peak values. Cassegrain focus.

- a) Observing far East: strong right-hand sidelobe;
- b) Symmetric beam not on meridian, but about 2^{h} East of it;
- c) Observing far West: strong left-hand sidelobes.



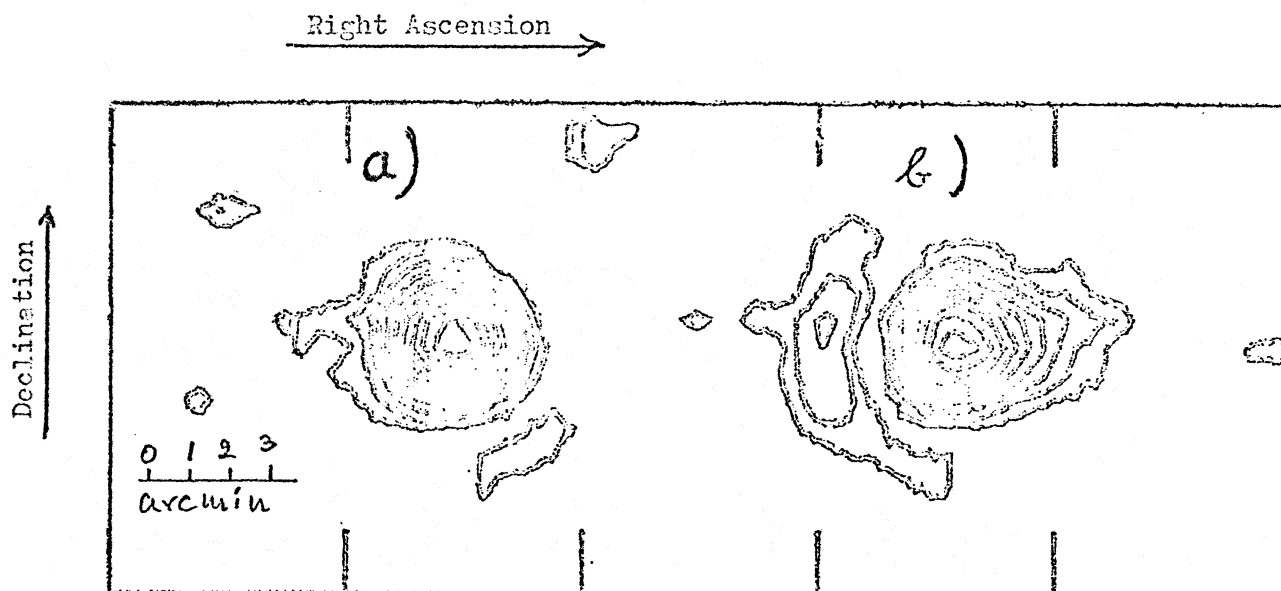


Fig. 3. Beam mapping with a two-feed receiver at prime focus, $\lambda = 2.04$ cm (14.7 GHz). The source is 3C 84, at declination $D = +41.3^\circ$, observed at $H = +3^{\text{h}} 04^{\text{m}}$ West. At this hour angle, the offset feed gives a better performance than the centered feed.

a) Offset feed, at 7.62 cm East of center; peak = 74 K.

b) Feed at center of Sterling mount; peak = 62 K, sidelobe = 10 K.

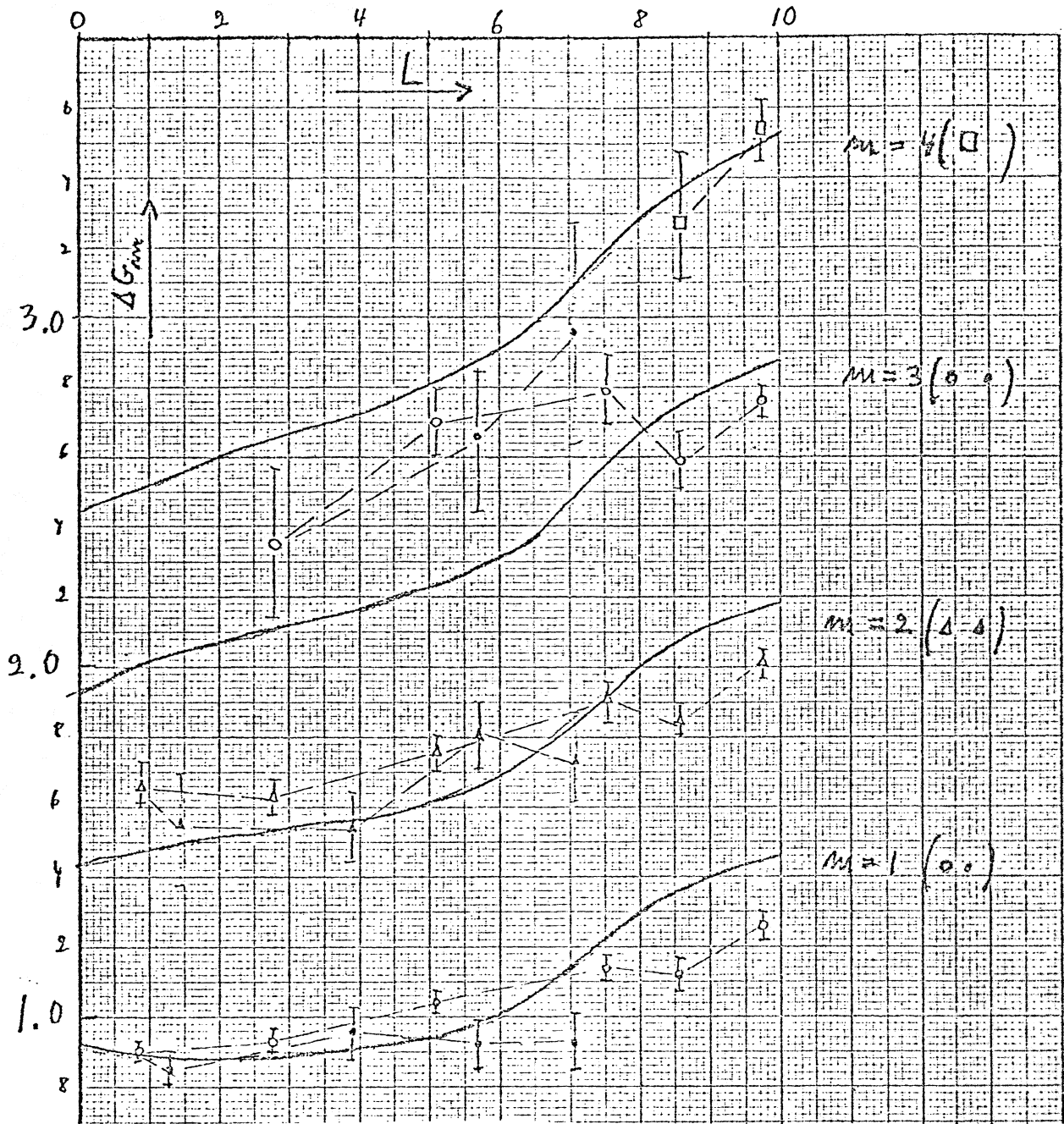


Fig. 4. Separation of sidelobes, observation (---) and theory (——). Open symbols for left-hand lobes observing West of H_0 , filled symbols for right-hand lobes observing East of H_0 . Used are $H_0 = -0^h 33^m$ and $\lambda_0 = 10.58$ cm, the best-fit values for this graph. Same observations as Fig. 1.

L = lateral feed offset, normalized with equation (12).

ΔG_m = angular distance of m -th sidelobe from main beam, see equations (13) and (16).

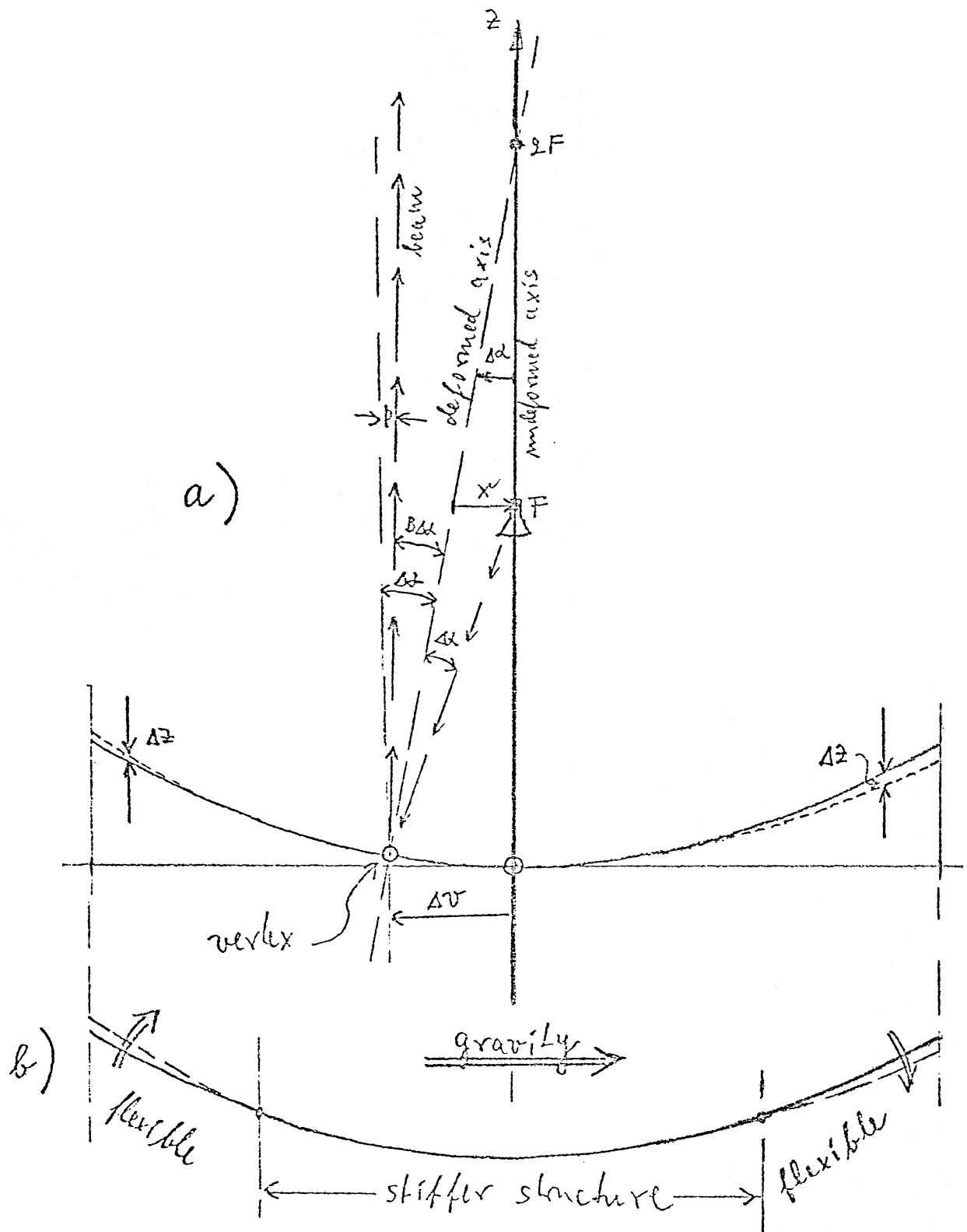


Fig. 5. Gliding rotation of the best-fit parabola, within a slightly deformed surface (---), rotating here about the point $2F$ on the axis.

- a) Small deformations Δz can cause a large feed offset x^* ; but the resulting pointing deviation $p = (1-B)\Delta\alpha$ is still small (B = beam deviation factor).
- b) This effect will take place whenever the rim is more flexible than the central part of the backup structure.